Newman[10] recommended having a full-time head-down PFD always in view, unless mission requirements dictated otherwise. If it is not feasible to have a full-time head-down PFD, the head-down display should be recalled by a single button push (without the need for the pilot to remove his hands from the controls). This approach has also been adopted by the military fixed-wing community.[7]

A HUD may not be suitable as a PFD in all flight conditions because the background may be too bright or distracting. Therefore it is felt that there needs to be a PFD available to the pilot. The issue is does it need to be up full time? This issue remains to be resolved.

Most existing civil HUDs do not replace the head-down PFD. The exception is the C-130J that was designed to allow the HUD to serve as the only visible PFD. The C-130J uses a yoke-mounted button for head-down PFD recall. The head-down PFD is also recalled automatically under certain circumstances.[15]

Application to Low-Level Operations with an HMD

In the case of NOE flight or transition to visual flight, the pilot may not have the time available to look inside, particularly during night or adverse weather operations. Of particular importance in the low-level environment is the assessment of the aircraft trajectory relative to obstructions. In this instance the HMD would be the de facto PFD. Clearly, it would be the only flight display being used.

As stated earlier, HUD studies recommended full-time display of the head-down PFD at all times.[10] This is an excessive requirement for HMDs because the purpose of the HMD is too allow the pilot to look off-axis and, as a result, he would probably not be able to see the head-down PFD.

However, it is our opinion that similar arrangements should apply to the use of an HMD, i.e., there should always be a head-down PFD available that is not necessarily displayed at all times.

Acknowledgment

This work was partially sponsored by Aeroflightdynamics Directory, NASA Ames Research Center, Moffett Field, California under Contract NAS2-14151. Wendell Stephens served as the Technical Monitor.

References

[1]"Transport Category Airplane Electronic Display Systems," Federal Aviation Administration, AC-25-11, July 1987.

[2]Barnette, J. F., "Role of Head-Up Display in Instrument Flight," U.S. Air Force Instrument Flight Center, LR-76-2, Randolph AFB, TX, Aug. 1976.

[3]Klopfstein, G., "Rational Study of Aircraft Piloting," *Intrados*, Thomson-CSF, Paris, 1966.

[4]Newman, R. L., "Operational Problems Associated with Head-Up Displays During Instrument Flight," U.S. Air Force Aerospace Medical Research Lab., TR-80-116, Wright–Patterson AFB, OH, Oct. 1980.

[5]Anderson, M. W., French, D. D., Newman, R. L., and Phillips, M. R., "Flight Testing a General Aviation Head-Up Display," *Journal of Aircraft*, Vol. 33, No. 1, 1996, 235–238.

[6]Hall, J. R., Stephens, C. M., and Penwill, J. C., "A Review of the Design and Development of the RAE Fast-Jet Head-Up Display Format," Royal Aircraft Establishment, FM-WP(89)-034, July 1989.

[7]"Military Standard: Aircraft Display Symbology," MIL-STD-1787B, Sept. 1989.

[8]"System Design and Analysis," Federal Aviation Administration, AC-25.1309-1A, June 1988.

[9]Haworth, L. A., and Newman, R. L., "Techniques for Evaluating Flight Displays," U.S. Army Aviation Systems Command, TR-92-A-006, Feb. 1993; also NASA TM-103947, Feb. 1993.

[10]Newman, R. L., "Head-Up Displays: Designing the Way Ahead," Avebury Aviation, Aldershot, England, UK, 1995.

[11]Newman, R. L., "Improvement of Head-Up Display Standards. I. Head-Up Display Design Guide," Vol. 1, U.S. Air Force Wright Aeronautical Labs., TR-87-3055, June 1987.

[12]Weintraub, D. J., and Ensing, M. J., "Human Factors Issues in Head-Up Display Design: The Book of HUD," Crew Systems Ergonomics Research Information Analysis Center, SOAR-92-2, Wright–Patterson AFB, OH, May 1992.

[13]Foyle, D. C., McCann, R. S., Sanford, B. D., and Schwirtzke, M. F. J., "Attentional Effects with Superimposed Symbology: Implications for Head-Up Displays (HUD)," *Proceedings of the 37th Annual Meeting of the Human Factors and Ergonomics Society* (Seattle, WA), Human Factors and Ergonomics Society, Santa Monica, CA, 1993, pp. 1340–1344.

[14]Ercoline, W. R., "Head-Up Displays: the Good, the Bad, and the Ugly," *Proceedings of the AGATE Human Factors Workshop on Flight Deck Design*, edited by K. W. Williams, Federal Aviation Administration, TM-AAM-500-96-12, Civil Aeromedical Inst., Oklahoma City, OK, 1996, pp. 36–40.

[15]"Crew Systems Design Document for the C-130J," Lockheed Martin Corp., Rept. J11B11-0603, Marietta, GA, Jan. 1997.

Modeling Turbulence in the Presence of Adverse Pressure Gradients

M. S. Rao* and H. A. Hassan†
North Carolina State University, Raleigh, North Carolina 27695-7910

Introduction

In an attempt to model a recent set of experiments by Skare and Krogstad,[1,2] dealing with equilibrium boundary layers near separation, it became clear that the traditional k-ω model was unable to reproduce the data. Careful investigation of the data suggested that the diffusion term in the k equation behaves differently in the presence and absence of unfavorable pressure gradients. This led to the conclusion that an important diffusion mechanism was missing from the k equation, and so a new diffusion model is proposed.

The only term that requires modeling in the k equation is the diffusion term.[3] Traditionally, it is modeled as

$$\frac{1}{2}\,\rho\overline{u_i' u_i' u_j'} + \overline{p' u_j'} = -\mu_t \sigma^* \frac{\partial k}{\partial x_j} \tag{1}$$

where ρ is the density, k is the turbulent kinetic energy, μ_t is the turbulent viscosity, u_i' is the velocity fluctuation, p' is the pressure fluctuation, and σ^* is a model constant.

The applicability of this model near separation is evaluated for an incompressible flow. In the near-wall region, the Wilcox k-ω model reduces to

$$0 = -\frac{\partial P}{\partial x} + \frac{\partial \tau}{\partial y} \tag{2}$$

$$0 = \frac{\partial}{\partial y}\left[\sigma^* \nu_t \frac{\partial k}{\partial y}\right] + \nu_t \left(\frac{\partial U}{\partial y}\right)^2 - \beta^* \omega k \tag{3}$$

$$0 = \frac{\partial}{\partial y}\left[\sigma_t \frac{\partial \omega}{\partial y}\right] + \alpha \left(\frac{\partial U}{\partial y}\right)^2 - \beta \omega^2 \tag{4}$$

Received April 29, 1996; presented as Paper 96-2429 at the AIAA 14th Applied Aerodynamics Conference, New Orleans, LA, June 14–20, 1996; revision received Jan. 6, 1998; accepted for publication Jan. 9, 1998. Copyright © 1998 by the American Institute of Aeronautics and Astronautics, Inc. All rights reserved.

*Research Assistant, Mechanical and Aerospace Engineering. Student Member AIAA.

†Professor, Mechanical and Aerospace Engineering. Associate Fellow AIAA.

where the turbulent eddy viscosity is defined as

$$\nu_t = k/\omega \tag{5}$$

P is the pressure, τ is the shear stress, U is the mean velocity, and ω is the specific dissipation rate. The values of the model constants are

$$\alpha = \tfrac{5}{9}, \quad \beta = \tfrac{3}{40}, \quad \beta^* = \tfrac{9}{100}, \quad \sigma^* = \tfrac{1}{2}, \quad \sigma = \tfrac{1}{2} \tag{6}$$

Integration of Eq. (2) gives

$$\tau = \tau_w + y\frac{\partial P}{\partial x} \simeq \mu_t \frac{\partial U}{\partial y} \tag{7}$$

where τ_w is the wall shear stress. In regions where $\tau_w \to 0$, Stratford[4] showed that U has the form

$$U = \frac{2(\sqrt{P'y})}{K_0}, \qquad P' = \frac{1}{\rho}\frac{\partial P}{\partial x} \tag{8}$$

where K_0 is typically a constant of about 0.51. Equation (8) was later confirmed by Townsend[5] using the data of Schubauer and Klebanoff.[6] In the limit of vanishing shear stress, Eqs. (7) and (8) give

$$\nu_t = K_0 P'^{1/2} y^{3/2} \tag{9}$$

When Eqs. (8) and (9) are substituted into Eqs. (3) and (4), the system yields two equations in two unknowns. Solution of these equations reveals the asymptotic behavior of k and ω in the region near separation. The result can be represented as[7]

$$k = Ay^m, \qquad \omega = By^n \tag{10}$$

where

$$m = 1, \quad n = -\frac{1}{2}, \quad A = \left(\frac{\alpha}{\beta}\right)^{1/2} P', \quad B = \frac{1}{K_0}\left(\frac{\alpha}{\beta}\right)^{1/2} P'^{1/2} \tag{11}$$

$$\frac{3}{2}\left(\frac{\alpha}{\beta}\right)^{1/2} \sigma^* K_0 + \frac{1}{K_0} - \frac{\alpha\beta^*}{K_0\beta} = 0 \tag{12}$$

Noting that

$$\alpha(\beta^*/\beta) = \tfrac{2}{3} \tag{13}$$

Eq. (12) reduces to

$$\frac{3}{2}\left(\frac{\alpha}{\beta}\right)^{1/2} \sigma^* K_0 + \frac{1}{3K_0} = 0 \tag{14}$$

In view of Eq. (6), the preceding result is a contradiction. This shows that the current modeling of diffusion is inadequate in a region near separation.

To remedy the preceding situation, we supplement diffusion with an additional term. The proposed modeling of the diffusion term is

$$\frac{1}{2}\rho\overline{u_i' u_i' u_j'} + \overline{p' u_j'} = -\mu_t\left[\sigma^*\frac{\partial k}{\partial x_j} + \sigma_p^*\frac{b_{ij}}{\rho}\frac{\partial P}{\partial x_j}\right] \tag{15}$$

where

$$b_{ij} = (\tau_{ij}/\rho k) + \tfrac{2}{3}\delta_{ij}, \qquad \tau_{ij} = -\rho\overline{u_i' u_j'} \tag{16}$$

and σ_p^* is a model constant. This model constant is determined from an analysis similar to the one performed in the preceding text. Using the standard k-ω notation, it can be shown that

$$\sigma_p^* = -\sigma^*(\alpha/\beta) - (2/9K_0^2)(\alpha/\beta)^{1/2} \simeq -6.03 \tag{17}$$

for $K_0 = 0.51$. Note that σ_p^* is negative, and so the new term is a negative diffusion term in the near-wall region for an adverse pressure gradient. It should be pointed out that the Stratford limit is valid in the near-wall region where $\tau_w \to 0$. The flow under consideration is attached. Thus the value presented in Eq. (17) is to be treated as a crude estimate of σ_p^*. After computations were made for a strong adverse pressure gradient flow, we set $\sigma_p^* = -5.13$ to best match the experiment.

It should be noted that Saffman[8] attempted to reproduce the Stratford limit using his k-ω^2 model. He found that for his model to reproduce Eq. (8), the various model constants had to take on imaginary values. The same can be shown for the k-ε model.

Results and Discussion

A boundary-layer code[9] is employed in carrying out the computations. A standard k-ω model and a modified k-ω model were implemented in the code.

The experiments of Refs. 1 and 2 represent an equilibrium boundary layer in a strong adverse pressure gradient flow at a Reynolds number per length of approximately 1.2×10^6. An equilibrium flow exhibits similarity in the outer region of the boundary layer.[5] The equilibrium region is maintained between $x_c = 4$ and 5 m. The strength of the pressure gradient is measured by the nondimensional pressure gradient parameter

$$\beta_T = \frac{\delta^*}{\tau_w}\frac{\partial P}{\partial x} \tag{18}$$

where δ^* is the displacement thickness. An average value of $\beta_T = 20$ was maintained in the equilibrium region.

To mimic the conditions stipulated by Stratford, the added diffusion term was implemented in the boundary-layer code as

$$\chi H(\chi) \tag{19}$$

where

$$\chi = \frac{\partial}{\partial x_i}\left[\mu_t\frac{b_{ij}}{\rho}\frac{\partial P}{\partial x_j}\right] = \frac{\partial}{\partial y}\left(\frac{k}{\omega^2}\frac{\partial U}{\partial y}\frac{\partial P}{\partial x}\right) \tag{20}$$

$H(\chi)$ is the Heaviside function, i.e., $H(\chi) = 1$ for $\chi > 0$ and is zero otherwise.

Skin friction values are compared in Fig. 1. Skin friction is defined as

$$C_{f,e} = \tau_w/\tfrac{1}{2}\rho_e U_e^2 \tag{21}$$

where subscript e denotes the edge of the boundary layer. k-ω results are about 50% higher than the expected results. The new model matches the data quite well with only a slight underprediction in the equilibrium pressure region of approximately 10%.

Figure 2 shows a representative shear stress $-\overline{u'v'}/u_\tau^2$ in the boundary layer at two of the six measurement stations, where

$$u_\tau^2 = \tau_w/\rho \tag{22}$$

The peak of the shear stress is at approximately $y/\delta = 0.5$. In a zero-pressure gradient flow, the maximum shear stress is at the wall. The modified k-ω results match the data quite well for $y/\delta \le 0.5$ and only slightly overpredict the outer region. Both methods find the correct location of the peak, but the magnitude is consistently underpredicted by the k-ω model. Based on these results and those of Ref. 7, we notice that τ_w, as determined by the original k-ω model, is greatly overestimated in regions of strong adverse pressure gradients.

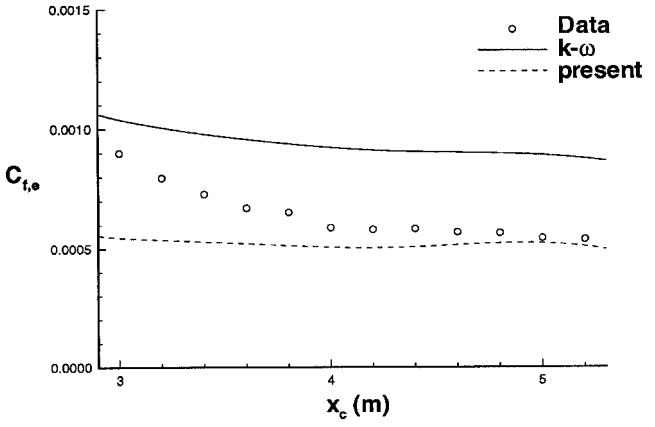

Fig. 1 Comparison of skin friction calculations with experiment.

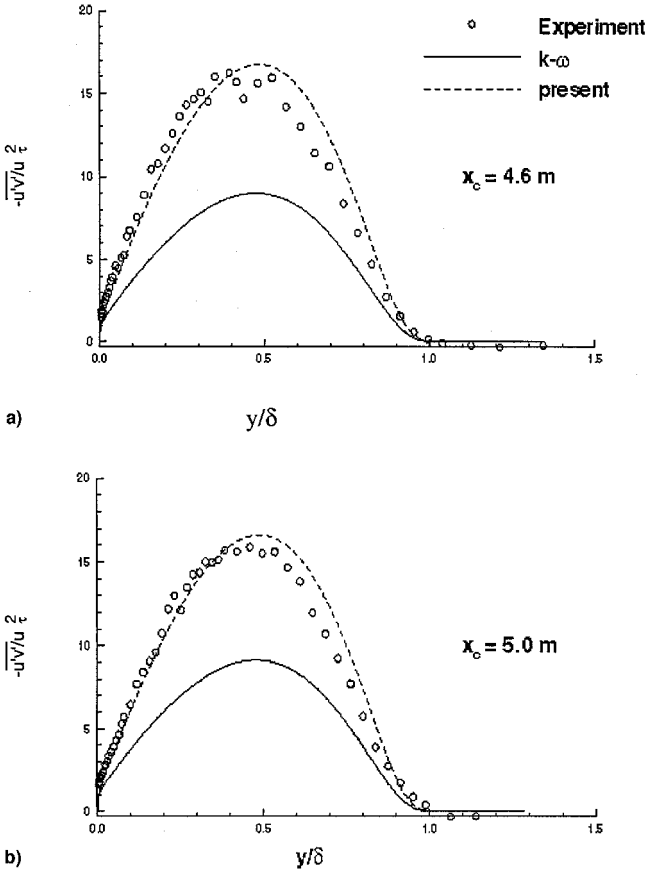

Fig. 2 Comparison of shear-stress profiles with experiment.

Concluding Remarks

This work identifies inadequate diffusion modeling as the cause for the inability to model separated flows or flows on the verge of separation. The results suggest that a new diffusion mechanism needs to be introduced in the k equation to explain observed behavior of turbulent flows in the presence of strong adverse pressure gradients at low speeds. The current modification of the k-ω model with an additional diffusion term based on the pressure gradient showed good agreement with the experiment when strong adverse pressure gradients exist in an incompressible flow.

Acknowledgments

The authors express their sincere appreciation to Per-Age Krogstad for providing them with his digitized data and a copy of Per Egil Skare's Ph.D. dissertation. Computer resources were provided by the North Carolina Supercomputing Center.

References

[1]Skare, P. E., and Krogstad, P. A., "A Turbulent Equilibrium Boundary Layer near Separation," *Journal of Fluid Mechanics*, Vol. 272, Aug. 1994, pp. 319–348.

[2]Krogstad, P. A., and Skare, P. E., "Influence of a Strong Adverse Pressure Gradient on the Turbulent Structure in a Boundary Layer," *Physics of Fluids*, Vol. 7, No. 8, 1995, pp. 2014–2024.

[3]Wilcox, D. C., "Turbulence Modeling in CFD," DCW Industries, Inc., La Canada, CA, 1993.

[4]Stratford, B. S., "The Prediction of Separation of Turbulent Boundary Layers," *Journal of Fluid Mechanics*, Vol. 5, Pt. 1, 1959, pp. 1–16.

[5]Townsend, A. A., "Equilibrium Layers and Wall Turbulence," *Journal of Fluid Mechanics*, Vol. 11, Pt. 1, Aug. 1961, pp. 97–120.

[6]Schubauer, G. B., and Klebanoff, P. S. "Investigation of Separation of the Turbulent Boundary Layer," NACA Rept. 1030, 1951.

[7]Rao, M. S., and Hassan, H. A., "Modeling Turbulence in the Presence of Adverse Pressure Gradients," AIAA Paper 96-2429, June 1996.

[8]Saffman, P. G., "A Model for Inhomogeneous Turbulent Flow," *Proceedings of the Royal Society of London, Series A: Mathematical and Physical Sciences*, Vol. A317, 1970, pp. 417–433.

[9]Harris, J. E., and Blanchard, D. K., "Computer Program for Solving Laminar, Transitional, or Turbulent Compressible Boundary Layer Equations for Two-Dimensional and Axisymmetric Flow," NASA TM 83207, Feb. 1982.

Buckling Analysis of Laminated Fiber-Reinforced Doubly Curved Shallow Shells

Maher N. Bismarck-Nasr*
Instituto Tecnolòǵico de Aeronàutica, São Josè dos Campos, SP, 12228-900, Brazil

I. Introduction

LAMINATED fiber-reinforced composite materials are increasingly used in aeronautical and space vehicles structures as shallow shell structural elements because of their high strength-to-weight ratio. However, their use in the design introduces several complicating factors that are not present in the conventional isotropic material constructions. Such complications are mainly a result of the fiber orientation, the number of layers used, and their stacking sequence. For efficient use, a good understanding of modern materials' construction is needed and their structural stability behavior under various loads and boundary conditions need to be studied. Because of the introduction of the geometric matrix concept by Gallagher and Padlog[1] and Kapur and Hartz,[2] many authors exploited the application of the finite element method for the analysis of linear and nonlinear buckling of plate and shell structures.[3–10] In most of the earlier works on the elastic stability analysis of plates and shells, the total potential energy functional was used for the finite element formulation of the problem. Alternatively, the problem can be formulated using a two-field, variable-modified functional with the transverse displacement w and Airy stress function F as the field variables of the problem. In Ref. 11, starting from Reissner's variational equation for free vibration of thin isotropic cylindrical curved plates, the Euler–Lagrange equations governing the problem and the boundary conditions were obtained. It was shown that the boundary con-

Received May 10, 1997; revision received Oct. 10, 1997; accepted for publication Nov. 9, 1998. Copyright © 1998 by the American Institute of Aeronautics and Astronautics, Inc. All rights reserved.

*Professor, Division of Aeronautical Engineering. Member AIAA.